Original Research

Sabine Goldberg*
Nadine J. Kabengi

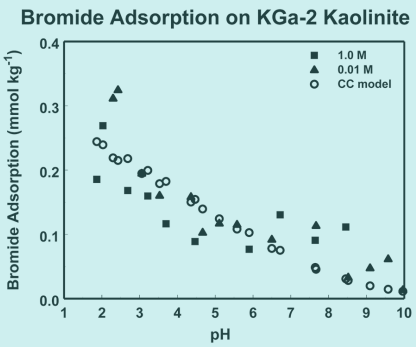

Bromide adsorption as a function of solution pH and background electrolyte concentration was determined for a set of reference minerals and soils. Adsorption was observed for pH <7, indicating that bromide would not act as a conservative tracer for such conditions. Therefore caution is advised when using bromide as a tracer under such conditions.

S. Goldberg, USDA-ARS, U.S. Salinity Lab., 450 W. Big Springs Rd., Riverside, CA 92507. N.J. Kabengi, Plant and Soil Sciences Dep., Univ. of Kentucky, Lexington, KY 40546. *Corresponding author (Sabine.Goldberg@ars.usda.gov).

Vadose Zone J. 9:780–786
doi:10.2136/vzj2010.0028
Received 16 Feb. 2010.
Published online 3 Aug. 2010.

Bromide Adsorption by Reference Minerals and Soils

Bromide, Br^-, adsorption behavior was investigated on amorphous Al and Fe oxide, montmorillonite, kaolinite, and temperate and tropical soils. Bromide adsorption decreased with increasing solution pH with minimal adsorption occurring above pH 7. Bromide adsorption was higher for amorphous oxides than for clay minerals. Shifts in point of zero charge (PZC) were observed on amorphous Al and Fe oxide following Br^- adsorption, suggesting an inner-sphere adsorption mechanism for Br^- on these surfaces. Ionic strength effects indicated an inner-sphere adsorption mechanism for Br^- on kaolinite and an outer-sphere adsorption mechanism on amorphous Fe oxide. Two chemical surface complexation models, the constant capacitance model and the triple layer model, were able to describe Br^- adsorption as a function of solution pH on all materials. For the oxides and clay minerals and most of the soils the fit of the constant capacitance model, containing an inner-sphere adsorption mechanism, was improved over that of the triple layer model, containing an outer-sphere adsorption mechanism, as measured by the overall variance, V_Y. Bromide adsorption on amorphous Fe oxide as a function of solution pH and solution ionic strength was well described using the triple layer model. Our results indicate that Br^- would most likely not act as a conservative tracer at soil solution pH values below 7. Therefore, we suggest that researchers carefully evaluate the pH regime and mineralogy of their study site before assuming that Br^- can be applied as a conservative tracer for transport experiments.

Abbreviations: IOC, inorganic carbon; OC, organic carbon; PZC, point of zero charge.

A tracer is an identifiable substance that can be followed through the course of a physical, chemical, or biological process. An ideal hydrogeologic tracer is nontoxic, inexpensive, moves with the water, is easy to detect in trace amounts, is chemically stable for a desired length of time, is not present in large amounts in the water being studied, and is not sorbed by the solid medium through which the water moves (Davis et al., 1980). In temperate regions Br^- has been considered to be an ideal tracer (Skaggs et al., 2002) that moves conservatively through soils (Bowman, 1984; Jardine et al., 1988), with a retardation coefficient $R = 1$.

Nonconservative behavior ($R \neq 1$) of Br^- has sometimes been observed. The cause of tracer movement that is faster than water flow ($R < 1$) has been attributed to anion exclusion from conducting pores due to repulsion of Br^- by negative charges on soil surfaces (Gerritse and Adeney, 1992). Tracer movement that is slower than water flow ($R > 1$) has been attributed to Br^- adsorption on variably charged soil surfaces that have appreciable anion exchange capacity (Boggs and Adams, 1992; Ishiguro et al., 1992; Seaman et al., 1995; Li et al., 1995; Ritter et al., 2005; Wong and Wittwer, 2009). Methods of soil sampling and sample preparation of column experiments can significantly affect Br^- adsorption behavior (Boggs and Adams, 1992). The Br^- adsorbing surfaces in soils are considered to be Fe and Al oxides and kaolinite (Boggs and Adams, 1992; Duwig et al., 1999; Ritter et al., 2005). Bromide retardation on iron-coated sand columns was attributed to the ferrihydrite coating because transport of Br^- through uncoated quartz sand columns was conservative (Brooks et al. (1998). Bromide retardation increased because anion exchange capacity increased with decreasing pH below the PZC.

Very few studies of Br^- adsorption have been conducted on soils (Li et al., 1995), clay minerals (Weerasooriya and Wickramarathna, 1999), and oxides (Petkovic et al., 1994; Chubar et al., 2005). Bromide adsorption was observed on the spodic B_h horizon of a spodosol but not on the surface A or the sandy E horizons. The Freundlich adsorption equation was fit to the Br^- adsorption isotherm data (Li et al., 1995). Freundlich adsorption isotherm parameters were also obtained from Br^- transport data in variably charged sediments where tailing was observed (Korom, 2000). Bromide adsorption on kaolinite decreased with increasing solution pH in the range 4 to 8. The magnitude of

Br^- adsorption decreased with increasing solution ionic strength of the background electrolyte, and no adsorption was observed above the point of zero net proton charge at pH = 8.8 (Weerasooriya and Wickramarathna, 1999). These observations are both indicative of a weak, outer-sphere adsorption mechanism. Bromide adsorption on a double hydrous oxide, $Fe_2O_3 \cdot Al_2O_3 \cdot xH_2O$, decreased with increasing pH in the range 3 to 8.5. The mechanism of iodide adsorption on amorphous iron oxide was found to be outer-sphere using X-ray absorption near-edge structure spectroscopy (Nagata et al., 2009). The Br^- adsorption reaction was fast, being 50% complete in the first 10 min of reaction, and fit a pseudo-second-order kinetic model (Chubar et al., 2005). Bromide adsorption on 2:1 clay minerals and simple oxides has not yet been investigated.

Surface complexation models are chemical models that have more general predictive capability than empirical adsorption isotherm equations. One such model, the triple layer model, has been applied to describe Br^- adsorption on Al oxide (Petkovic et al., 1994) and kaolinite (Weerasooriya and Wickramarathna, 1999). In both applications Br^- adsorption was considered to be nonspecific and described using an outer-sphere surface complexation mechanism. A major advantage of surface complexation models over adsorption isotherm equations is their ability to describe adsorption as a function of solution pH.

The objectives of this study were (i) to determine Br^- adsorption behavior on Al and Fe oxides, kaolinite, montmorillonite, and temperate and tropical soils as a function of solution pH and (ii) to evaluate the ability of two chemical surface complexation models, the constant capacitance model and the triple layer model, to describe Br^- adsorption on these surfaces as a function of solution pH.

Materials and Methods

Bromide adsorption behavior was studied on various adsorbents. Amorphous Al and Fe oxides were synthesized using the method of Sims and Bingham (1968). Aluminum oxide was synthesized by neutralizing 0.41 M $AlCl_3$ with an equal part of 1.1 M NaOH. In the Fe oxide synthesis, 100 mL of 1.5 M $FeCl_3$ were neutralized with 225 mL of 2.0 M NaOH. The amorphous oxides were air-dried and gently crushed. X-ray diffraction powder analyses verified that the oxides were amorphous and contained no crystalline impurities. Samples of SWy-1 Na-montmorillonite and KGa-2 kaolinite were obtained from the Clay Minerals Society's Source Clay Repository (University of Missouri, Columbia) and used without pretreatment. X-ray diffraction analysis found trace impurities of mica and chlorite in the montmorillonite and the kaolinite, respectively. Surface areas of the oxides and clays were determined from single-point Brunauer–Emmett–Teller N_2 adsorption isotherms. Surface area was 67.5 $m^2\ g^{-1}$ for the Al oxide, 184 $m^2\ g^{-1}$ for the Fe oxide, 31.6 $m^2\ g^{-1}$ for the montmorillonite, and 19.3 $m^2\ g^{-1}$ for the kaolinite.

Points of zero charge for the amorphous Al and Fe oxides were determined by microelectrophoresis using a Zeta-Meter 3.0 system (Zeta Meter, Long Island City, NY). The electrophoretic mobilities of suspensions containing 0.01% oxide in 0.015 M NaCl were determined at various pH values. Points of zero charge were obtained by linear interpolation to zero electrophoretic mobility. Electrophoretic mobility measurements were also determined in the presence of 10 and 20 mg $Br^-\ L^{-1}$.

Bromide adsorption was investigated on the <2-mm fraction of four temperate and four tropical soils. The temperate soil samples consisted of the A horizons of four soil series from Oklahoma, USA. The Dennis, Kirkland, and Summit soils are Mollisols and the Osage soil is a Vertisol. The four tropical soils are clayey Oxisols from Brazil. Soil chemical characteristics are presented in Table 1. Soil surface areas were obtained using ethylene glycol monoethyl ether adsorption (Cihacek and Bremner, 1979). Free Fe and Al oxides were determined as described by Coffin (1963). Organic carbon (OC) and inorganic carbon (IOC) contents were determined by carbon coloumetry. Total carbon was quantified by combustion at 950°C, IOC was analyzed using an acidification module and heating, and OC was determined by difference. Cation exchange capacities of the U.S. soils were measured by sodium saturation and magnesium extraction as described by Rhoades (1982) for arid land soils. Cation and anion exchange capacities of the Brazilian soils were determined by compulsive exchange using barium chloride saturation and magnesium sulfate extraction (Gillman and Sumpter, 1986).

Table 1. Classifications and chemical characteristics of soils.

Soils	Depth	pH	CEC	AEC	SA	IOC	OC	Fe	Al
	cm		— $mmol_c\ kg^{-1}$ —		$m^2\ g^{-1}$	——— $g\ kg^{-1}$ ———			
Dennis (fine, mixed thermic Aquic Argiudoll)	A	5.2	85.5		40.3	0.0014	18.6	12.9	1.7
Kirkland (fine, mixed, superactive, thermic Udertic Paleustoll)	A	5.0	154		42.1	0.014	12.3	5.6	0.80
Osage (fine, smectitic, thermic Typic Epiaquert)	A	6.8	377		134	0.59	29.2	15.9	1.4
Summit (fine, smectitic, thermic Oxyaquic Vertic Argiudoll)	A	6.3	374		218	0.25	26.7	16.2	2.3
Red oxisol: Argila clay S1		6.2	91.4	4.07	31.6	<0.001	1.9	27.0	1.32
Red oxisol: Argila clay S2		6.6	11.9	1.04	44.1	<0.001	2.3	28.5	1.64
Yellow Oxisol	30	4.3	279	2.02	64.5	<0.001	28.1	43.7	8.82
Yellow Oxisol	35	4.9	77.8	6.60	22.8	<0.001	0.68	41.9	1.75

Bromide adsorption experiments were performed in batch systems to determine adsorption envelopes, the amount of Br^- adsorbed as a function of solution pH per fixed total Br^- concentration. Soil samples were used without any pretreatment. Samples of adsorbent (0.1 g for oxides, 0.75 g for montmorillonite, 2.5 g for kaolinite, and 5.0 g for soils) were added to 50-mL polypropylene centrifuge tubes and equilibrated with 25 mL of a 0.1 M $NaNO_3$ solution by shaking for 20 h on a reciprocating shaker. A background electrolyte is necessary because the constant capacitance model assumes a constant ionic medium reference state. This solution contained 20 mg Br^- L^{-1} and had been adjusted to the desired pH range of 3 to 8 using 1 M HNO_3 or 1 M NaOH. Acid or base additions changed the total volumes by <2%. Additional adsorption experiments were performed in a background electrolyte of 0.01 M or 1.0 M $NaNO_3$ using amorphous Fe oxide and kaolinite. After reaction, the samples were centrifuged and the decantates analyzed for pH, filtered, and analyzed for Br^- concentration using a Technicon Auto Analyzer II and the fluorescein method of Marti and Arozarena (1981).

Detailed discussions of the theory and assumptions of the constant capacitance and triple layer models are provided in Goldberg (1992). In the application of the constant capacitance model to Br^- adsorption the following surface complexation constants were considered:

$$SOH_{(s)} + H^+_{(aq)} \leftrightarrow SOH^+_{2(s)} \quad [1]$$

$$SOH_{(s)} \leftrightarrow SO^-_{(s)} + H^+_{(aq)} \quad [2]$$

$$SOH_{(s)} + Br^-_{(aq)} + H^+_{(aq)} \leftrightarrow SBr_{(s)} + H_2O \quad [3]$$

where SOH represents reactive surface hydroxyls on oxide minerals and aluminols on clay mineral edges.

Intrinsic equilibrium constants for the surface complexation reactions are:

$$K_+(\text{int}) = \frac{[SOH^+_2]}{[SOH][H^+]}\exp(F\psi/RT) \quad [4]$$

$$K_-(\text{int}) = \frac{[SO^-][H^+]}{[SOH]}\exp(-F\psi/RT) \quad [5]$$

$$K^{\text{is}}_{\text{Br}}(\text{int}) = \frac{[SBr]}{[SOH][Br^-][H^+]} \quad [6]$$

where square brackets indicate concentrations (mol L^{-1}), F is the Faraday constant (C mol_c^{-1}), ψ is the surface potential (V), R is the molar gas constant (J mol^{-1} K^{-1}), T is the absolute temperature (K), and "is" stands for inner-sphere. The exponential terms can be considered as solid-phase activity coefficients that correct for surface charges.

Mass balance of the surface functional group is:

$$[SOH]_T = [SOH] + [SOH^+_2] + [SBr] \quad [7]$$

where $[SOH]_T$ is related to the surface site density, N_s, by:

$$[SOH]_T = \frac{S_A C_p 10^{18}}{N_A} N_s \quad [8]$$

where S_A is the surface area (m^2 g^{-1}), C_p is the particle concentration (g L^{-1}), N_A is Avogadro's number, and N_s has units of (sites nm^{-2}).

Charge balance is:

$$\sigma = [SOH^+_2] - [SO^-] \quad [9]$$

where σ is the surface charge (mol_c L^{-1}). The relationship between surface charge and surface potential is:

$$\sigma = \frac{CS_A C_p}{F}\psi \quad [10]$$

where C is the capacitance (F m^{-2}).

In the present application of the triple layer model to Br^- adsorption the following surface complexation constants were considered in addition to the protonation and dissociation reactions, Eq. [1] and [2]:

$$SOH_{(s)} + Na^+_{(aq)} \leftrightarrow SO^- - Na^+_{(s)} + H^+_{(aq)} \quad [11]$$

$$SOH_{(s)} + H^+_{(aq)} + NO^-_{3(aq)} \leftrightarrow SOH^+_2 - NO^-_{3(s)} \quad [12]$$

The inner-sphere Br^- surface complexation reaction, Eq. [3], is replaced by an outer-sphere surface complexation reaction:

$$SOH_{(s)} + Br^-_{(aq)} + H^+_{(aq)} \leftrightarrow SOH^+_2 - Br^-_{(s)} \quad [13]$$

Intrinsic equilibrium constants for the surface complexation reactions are Eq. [4] and [5] and:

$$K_{C^+}(\text{int}) = \frac{[SO^- - Na^+][H^+]}{[SOH][Na^+]}\exp[F(\psi_\beta - \psi_o)/RT] \quad [14]$$

$$K_{A^-}(\text{int}) = \frac{[SOH^+_2 - NO^-_3]}{[SOH][H^+][NO^-_3]}\exp[F(\psi_o - \psi_\beta)/RT] \quad [15]$$

$$K^{\text{os}}_{\text{Br}}(\text{int}) = \frac{[SOH^+_2 - Br^-]}{[SOH][Br^-][H^+]}\exp[F(\psi_o - \psi_\beta)/RT] \quad [16]$$

where "o" refers to the surface plane of inner-sphere adsorption, β refers to the plane of outer-sphere adsorption, and "os" stands for outer-sphere.

Mass balance of the surface functional group is:

$$[SOH]_T = [SOH] + [SOH_2^+] + [SO^-] + [SO^- - Na^+] + [SOH_2^+ - NO_3^-] + [SOH_2^+ - Br^-] \quad [17]$$

and the charge balances are:

$$\sigma_o + \sigma_\beta + \sigma_d = 0 \quad [18]$$

$$\sigma_o = [SOH_2^+] + [SOH_2^+ - NO_3^-] + [SOH_2^+ - Br^-] - [SO^-] - [SO^- - Na^+] \quad [19]$$

$$\sigma_\beta = [SO^- - Na^+] - [SOH_2^+ - NO_3^-] - [SOH_2^+ - Br^-] \quad [20]$$

where "d" refers to the plane of the diffuse ion swarm. The relationships between the surface charges and surface potentials are:

$$\sigma_o = \frac{C_1 S_A C_p}{F}(\psi_o - \psi_\beta) \quad [21]$$

$$\sigma_d = \frac{C_2 S_A C_p}{F}(\psi_d - \psi_\beta) \quad [22]$$

$$\sigma_d = \frac{S_A C_p}{F}(8\varepsilon_o DRTI)^{1/2} \sinh(F\psi_d / 2RT) \quad [23]$$

where C_1 and C_2 are capacitances, ε_o is the permittivity of a vacuum, D is the dielectric constant of water, and I is the ionic strength.

The computer program FITEQL 3.2 (Herbelin and Westall, 1996) was used to fit surface complexation constants to the experimental Br^- adsorption data. The program uses a nonlinear least squares optimization routine to fit equilibrium constants to experimental data and contains both the constant capacitance and the triple layer models of adsorption. The FITEQL code uses the overall variance, V, in Y as the goodness-of-fit criterion:

$$V_Y = \frac{SOS}{DF} \quad [24]$$

where SOS is the weighted sum of squares of the residuals, and DF is the degrees of freedom. In our applications of both models, the surface site density was set at 2.31 sites nm^{-2}, as was recommended by Davis and Kent (1990) for natural materials.

Other initial input parameter values for the constant capacitance model were capacitance: C = 1.06 F m^{-2} (considered optimum for Al oxide by Westall and Hohl, 1980) and protonation and dissociation constants: log K_+(int) = 7.31, log K_-(int) = −8.80 for amorphous Fe oxide, log K_+(int) = 7.38, log K_- (int) = −9.09 for amorphous Al oxide and clays, and log K_+(int) = 7.35, log K_- (int) = −8.95 for soils (obtained from a literature compilation of experimental values for Fe and Al oxides by Goldberg and Sposito, 1984).

Other input parameters for the triple layer model were capacitances: C_1 = 1.2 F m^{-2}, C_2 = 0.2 F m^{-2} (considered optimum for goethite by Zhang and Sparks, 1990) and surface complexation constants: log K_+(int) = 4.3, log K_- (int) = −9.8, log K_{C+}(int) = −9.3, log K_{A-}(int) = 5.4 for amorphous Fe oxide (obtained for goethite by Zhang and Sparks, 1990), and log K_+(int) = 5.0, log K_-(int) = −11.2, log K_{C+}(int) = −8.6, log K_{A-}(int) = 7.5 for amorphous Al oxide, clays, and soils (obtained for γ-Al_2O_3 by Sprycha, 1989a,b).

Results and Discussion

The PZC in the presence of a background electrolyte of 0.015 M NaCl was found to occur at pH 8.8 for amorphous Al oxide and pH 5.8 for amorphous Fe oxide. These PZC values are less than previous determinations using the same synthesis techniques (Goldberg et al., 1996). The differences in PZC values are due to recent problems with the electrophoretic mobility analyzer. The important observation for the purpose of the present investigation is not so much the absolute PZC value but whether a shift in PZC is observed on anion adsorption. Figures 1 and 2 present electrophoretic mobility vs. pH obtained for amorphous Al oxide and amorphous Fe oxide, respectively, on adsorption of Br^-. For both oxides the PZC values shifted to lower pH value in the presence of Br^- anions, although the shift for amorphous Fe oxide was small. Specific inner-sphere adsorption of ions produces PZC shifts and electrophoretic mobility reversals with increasing ion concentration (Hunter, 1981). These changes in PZC values are macroscopic evidence of inner-sphere surface complexation of Br^- on amorphous Al and Fe oxides. This observation suggests that Br^- is adsorbed more strongly on oxides than on kaolinite (Weerasooriya and Wickramarathna, 1999).

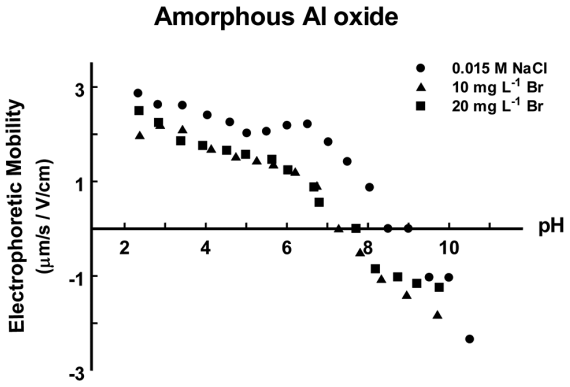

Fig. 1. Electrophoretic mobility of amorphous Al oxide as a function of pH and total Br^- concentration in 0.015 M NaCl solution. The circles represent zero Br^- treatment.

Bromide adsorption as a function of solution pH is indicated in Fig. 3a for amorphous Al oxide and in Fig. 3b for montmorillonite. Bromide exhibited decreasing adsorption with increasing pH with minimal adsorption occurring above pH 7 for both oxides and clays. The amorphous Fe oxide adsorbed 10 times as much Br^- as the montmorillonite, consistent with the high reactivity of this material for adsorption of other ions. The magnitude of Br^- adsorption on amorphous Al oxide was comparable to that on amorphous Fe oxide. The magnitude of Br^- adsorption on kaolinite was approximately one-half of that on montmorillonite, consistent with its smaller surface area and larger particle size.

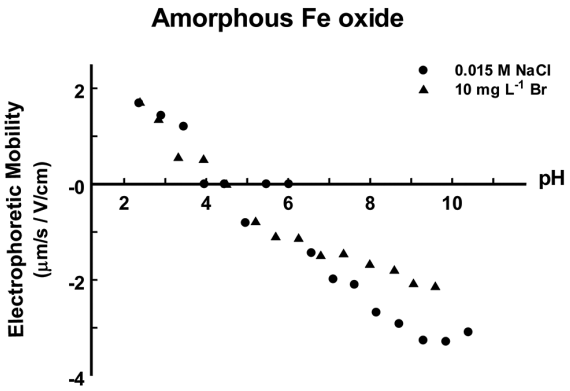

Fig. 2. Electrophoretic mobility of amorphous Fe oxide as a function of pH and total Br^- concentration in 0.015 M NaCl solution. The circles represent zero Br^- treatment.

Evaluation of the effect of changes in solution ionic strength on the extent of ion adsorption is another macroscopic method of inferring the ion adsorption mechanism. Ions that form outer-sphere surface complexes show decreasing adsorption with increasing solution ionic strength, while ions that form inner-sphere surface complexes show little ionic strength dependence or increasing adsorption with increasing solution ionic strength (McBride, 1997). The effect of ionic strength on Br^- adsorption is indicated in Fig. 4a for kaolinite and Fig. 4b for amorphous Fe oxide. Solution ionic strength varied by two orders of magnitude, from 0.01 to 1.0 M $NaNO_3$. Bromide adsorption on kaolinite exhibited little ionic strength dependence indicative of an inner-sphere adsorption mechanism. This result is in contrast to the outer-sphere adsorption mechanism observed for bromide adsorption on kaolinite (Weerasooriya and Wickramarathna, 1999). Bromide adsorption on amorphous Fe oxide exhibited pronounced ionic strength dependence indicative of an outer-sphere adsorption mechanism. This result is in agreement with the outer-sphere adsorption mechanism observed for iodide adsorption on amorphous Fe oxide (Nagata et al., 2009).

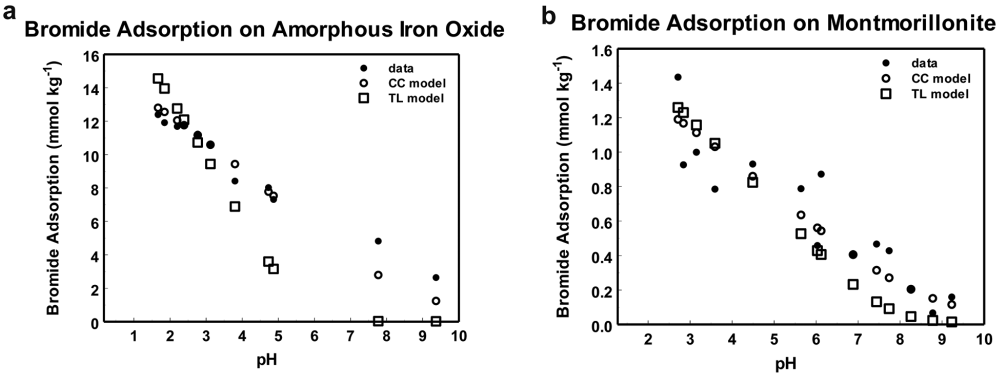

Fig. 3. (a) Bromide adsorption on amorphous Fe oxide as a function of solution pH from an equilibrating solution of Br = 20 mg L^{-1}. Experimental data are represented by solid circles. The constant capacitance model fit is represented by open circles. The triple layer model fit is represented by open squares. The distribution coefficient K_d ranges from 59 at low pH to 10.5 at high pH. (b) Bromide adsorption on montmorillonite as a function of solution pH from an equilibrating solution of Br = 20 mg L^{-1}. Experimental data are represented by solid circles. The constant capacitance model fit is represented by open circles. The triple layer model fit is represented by open squares. The distribution coefficient K_d ranges from 7.2 at low pH to 0.7 at high pH.

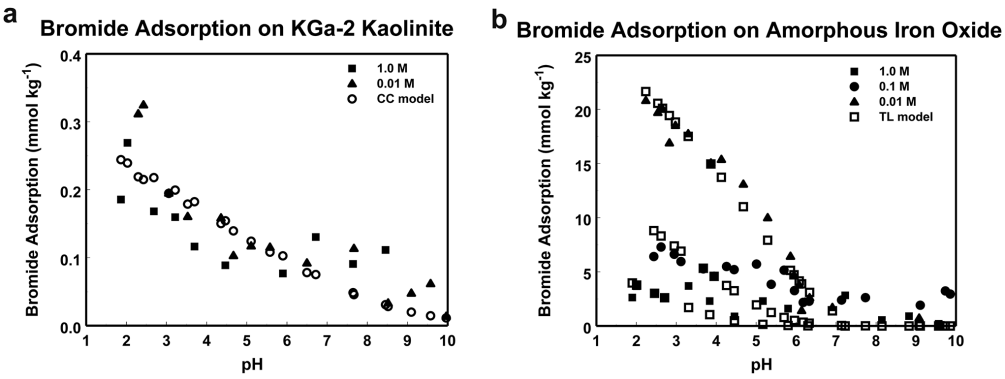

Fig. 4. (a) Bromide adsorption on kaolinite as a function of solution pH and solution ionic strength from an equilibrating solutions of $NaNO_3$ and Br = 20 mg L^{-1}. Experimental data are represented by solid symbols. The constant capacitance model fit is represented by open circles. (b) Bromide adsorption on amorphous Fe oxide as a function of solution pH and solution ionic strength from an equilibrating solutions of $NaNO_3$ and Br = 20 mg L^{-1}. Experimental data are represented by solid symbols. The triple layer model fit is represented by open squares.

Adsorption of Br^- on soil samples as a function of solution pH is indicated for two of the U.S. soils (Fig. 5a and 5b) and for two of

the Brazilian oxisols (Fig. 5c and 5d). Similar to the behavior of the oxides and clay minerals, Br^- adsorption on the soils decreased with increasing pH. Bromide adsorption on the oxisols was only about one-half as much as on the U.S. Mollisol, Kirkland, and the U.S. Vertisol, Osage. This behavior also holds for the other Brazilian and U.S. soils. This was surprising since the Fe oxide content of the oxisols was twice that of the U.S. soils. This observation would suggest that clay minerals play a major role in Br^- adsorption on the mollisols and the vertisol.

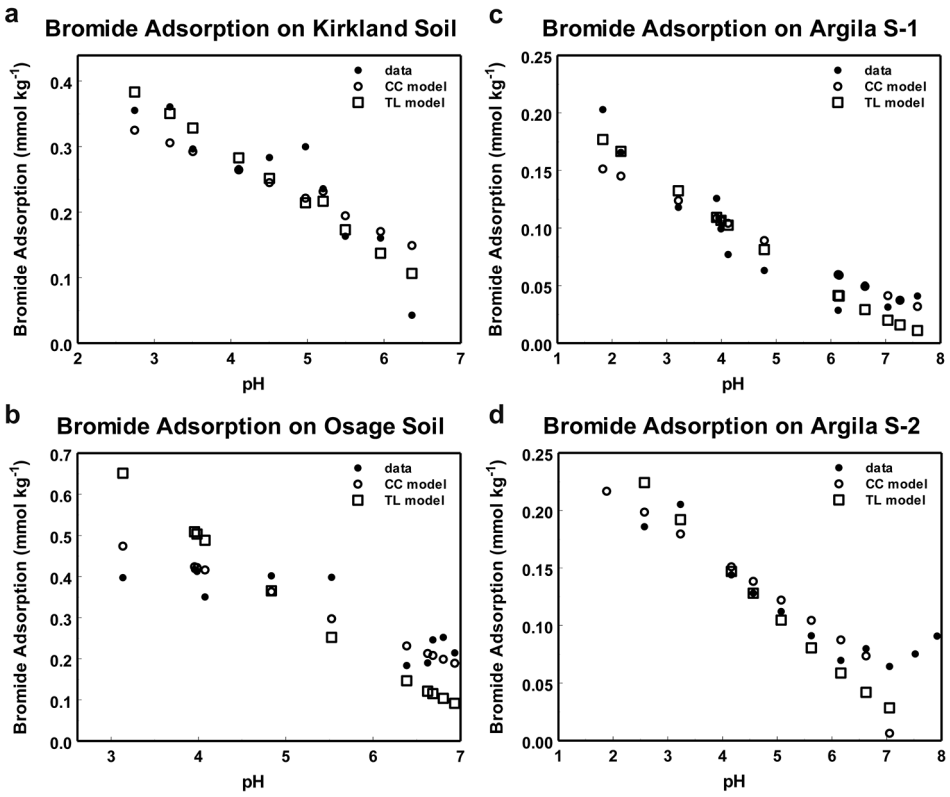

Fig. 5. (a) Bromide adsorption on Kirkland soil as a function of solution pH from an equilibrating solution of Br = 20 mg L^{-1}. Experimental data are represented by solid circles. The constant capacitance model fit is represented by open circles. The triple layer model fit is represented by open squares. The distribution coefficient K_d ranges from 2.1 at low pH to 0.2 at high pH. (b) Bromide adsorption on Osage soil as a function of solution pH from an equilibrating solution of Br = 20 mg L^{-1}. Experimental data are represented by solid circles. The constant capacitance model fit is represented by open circles. The triple layer model fit is represented by open squares. The distribution coefficient K_d ranges from 2.3 at low pH to 0.8 at high pH. (c) Bromide adsorption on Argila S-1 soil as a function of solution pH from an equilibrating solution of Br = 20 mg L^{-1}. Experimental data are represented by solid circles. The constant capacitance model fit is represented by open circles. The triple layer model fit is represented by open squares. The distribution coefficient K_d ranges from 0.9 at low pH to 0.1 at high pH. (d) Bromide adsorption on Argila S-2 soil as a function of solution pH from an equilibrating solution of Br = 20 mg L^{-1}. Experimental data are represented by solid circles. The constant capacitance model fit is represented by open circles. The triple layer model fit is represented by open squares. The distribution coefficient K_d ranges from 4 at low pH to 0.3 at high pH.

The surface complexation models were fit to the Br^- adsorption envelopes of all samples optimizing one Br surface complexation constant each: $\log K^{is}_{Br}(int)$ for the constant capacitance model and $\log K^{os}_{Br}(int)$ for the triple layer model. The optimized values of the Br surface complexation constants are provided in Table 2. For the oxides and clay minerals, the values of the goodness-of-fit criterion, V_Y, for the constant capacitance model are considerably smaller than those for the triple layer model. This is not surprising since the Br^- adsorption envelopes are described more closely by the constant capacitance model (see Fig. 3a for amorphous Fe oxide and Fig. 3b for montmorillonite). The improved fit with the constant capacitance model, which describes ion adsorption using an inner-sphere adsorption mechanism, is consistent with the ZPC shifts observed on amorphous Al and Fe oxides following Br^- adsorption (Fig. 1 and 2). Consistent with the small amount of ionic strength dependence, the constant capacitance model was well able to describe Br^- adsorption on kaolinite using an inner-sphere adsorption mechanism (see Fig. 4a). The pronounced ionic strength dependence observed on Br^- adsorption on amorphous Fe oxide (Fig. 4b) is in contrast to the PZC shift results and consistent with a triple layer model application using an outer-sphere adsorption mechanism. The triple layer model was able to describe the results well (see Fig. 4b).

For both surface complexation models, the average values of the Br adsorption constants for the U.S. soils are not statistically significantly different at the 95% level of confidence from the average values for the Brazilian soils (see Table 2). The ability of both models to describe Br^- adsorption on the soils is good and is shown in Fig. 5a through 5d. For five of the eight soils the magnitude of V_Y for the constant capacitance model is smaller than for the triple layer model, indicating an improved fit. The magnitudes of the $\log K^{is}_{Br}(int)$ values for the oxides and reference clays are larger than those for soils, suggesting a greater adsorption affinity for Br^- on these materials.

In prior studies, Br^- adsorption in acid soils and Andisols has been attributed to the presence of variable charge minerals such as Al and Fe oxides and kaolinite (Boggs and Adams, 1992; Seaman et al., 1995). Our experimental results for amorphous Al and Fe oxides, kaolinite, and montmorillonite have verified that these materials indeed adsorb Br^- at pH values below 8. Electrophoretic mobility experiments suggest that Br^- adsorption occurs via a specific inner-sphere adsorption mechanism on Al and Fe oxide. Ionic

Table 2. Surface complexation model constants.

	Constant capacitance model		Triple layer model	
Solid	Log K^{is}_{Br}(int)	V_Y	Log K^{os}_{Br}(int)	V_Y
Amorphous Fe oxide	9.36	68.2	6.73	128.
Amorphous Al oxide	9.87	47.4	9.08	80.1
Montmorillonite	9.44	25.5	8.62	46.5
Kaolinite	8.43	17.7	7.55	27.2
Dennis soil	8.86	18.2	8.04	109.
Kirkland soil	8.58	55.5	7.75	31.5
Osage soil	8.26	33.2	7.33	197.
Summit soil	7.82	60.9	6.77	30.8
Average U.S. soils	8.38 ± 0.44		7.47 ± 0.55	
Argila clay S1	8.21	12.1	7.35	12.4
Argila clay S2	8.23	6.8	7.35	14.1
Yellow Oxisol 0.30 m	7.72	22.2	6.82	12.8
Yellow Oxisol 0.35 m	8.20	29.2	7.35	35.1
Average Brazil soils	8.09 ± 0.25		7.21 ± 0.27	
Average all soils	8.24 ± 0.37		7.35 ± 0.42	

strength effects results suggest an inner-sphere adsorption mechanism on kaolinite and an outer-sphere adsorption mechanism on amorphous Fe oxide.

Our study showed Br^- adsorption on both temperate and tropical soils to occur at pH values below pH 7. These results indicate that Br^- would therefore most likely not act as a conservative tracer at soil solution pH values below 7. Since our experiments were conducted in the presence of 0.1 M NO_3^- concentration, Br^- adsorption in field situations, where the NO_3^- concentration and any competitive effect will be much less, would be expected to be even greater. We therefore suggest that researchers carefully evaluate the pH regime and mineralogy of their study site before assuming that Br^- can be applied as a conservative tracer for transport experiments.

Acknowledgments

Gratitude is expressed to Ms. K. Theel, Ms. P. Xiong, Mr. M. Follansbee, and Mr. H.S. Forster for technical assistance, Dr. N. Basta for providing the U.S. soil samples, and Dr. B. Pontedeiro for providing the Brazilian soil samples.

References

Boggs, J.M., and E.E. Adams. 1992. Field study of dispersion in a heterogeneous aquifer. 4. Investigation of adsorption and sampling bias. Water Resour. Res. 28:3325–3336.

Bowman, R.S. 1984. Evaluation of some new tracers for soil water studies. Soil Sci. Soc. Am. J. 48:987–993.

Brooks, S.C., D.L. Taylor, and P.M. Jardine. 1998. Thermodynamics of bromide exchange on ferrihydrite: Implications for bromide transport. Soil Sci. Soc. Am. J. 62:1275–1279.

Chubar, N.I., V.F. Samanidou, V.S. Kouts, G.G. Gallios, V.A. Kanibolotsky, V.V. Strelko, and I.Z. Zhuravlev. 2005. Adsorption of fluoride, chloride, bromide, and bromate ions on a novel ion exchanger. J. Colloid Interface Sci. 291:67–74.

Cihacek, L.J., and J.M. Bremner. 1979. A simplified ethylene glycol monoethyl ether procedure for assessing soil surface area. Soil Sci. Soc. Am. J. 43:821–822.

Coffin, D.E. 1963. A method for the determination of free iron oxide in soils and clays. Can. J. Soil Sci. 43:7–17.

Davis, J.A., and D.B. Kent. 1990. Surface complexation modeling in aqueous geochemistry. Rev. Mineral. 23:177–260.

Davis, S.N., G.M. Thompson, H.W. Bentley, and G. Stiles. 1980. Ground-water tracers—A short review. Ground Water 18:14–23.

Duwig, C., T. Becquer, B.E. Clothier, and M. Vauclin. 1999. A simple dynamic method to estimate anion retention in an unsaturated soil. C. R. Acad. Sci. Ser. II 328:759–764.

Gerritse, R.G., and J.A. Adeney. 1992. Tracers in recharge– effects of partitioning in soils. J. Hydrol. 131:255–268.

Gillman, G.P., and E.A. Sumpter. 1986. Modification to the compulsive exchange method for measuring exchange characteristics of soils. Aust. J. Soil Res. 24:61–66.

Goldberg, S. 1992. Use of surface complexation models in soil chemical systems. Adv. Agron. 47:233–329.

Goldberg, S., H.S. Forster, and C.L. Godfrey. 1996. Molybdenum adsorption on oxides, clay minerals, and soils. Soil Sci. Soc. Am. J. 60:425–432.

Goldberg, S., and G. Sposito. 1984. A chemical model of phosphate adsorption by soils. I. Reference oxide minerals. Soil Sci. Soc. Am. J. 48:772–778.

Herbelin, A.L., and J.C. Westall. 1996. FITEQL: A computer program for determination of chemical equilibrium constants from experimental data. Rep. 96-01. Version 3.2. Dep. of Chemistry, Oregon State University, Corvallis.

Hunter, R.J. 1981. Zeta potential in colloid science. Principles and applications. Academic Press, London.

Ishiguro, M., K.-C. Song, and K. Yuita. 1992. Ion transport in an allophanic andisol under the influence of variable charge. Soil Sci. Soc. Am. J. 56:1789–1793.

Jardine, P.M., G.V. Wilson, and R.J. Luxmoore. 1988. Modeling the transport of inorganic ions through undisturbed soil columns from two contrasting watersheds. Soil Sci. Soc. Am. J. 52:1252–1259.

Korom, S.F. 2000. An adsorption isotherm for bromide. Water Resour. Res. 36:1969–1974.

Li, Y.C., A.K. Alva, D.V. Calvert, and D.J. Banks. 1995. Adsorption and transport of nitrate and bromide in a spodosol. Soil Sci. 160:400–404.

Marti, V.C., and C.E. Arozarena. 1981. Automated colorimetric determination of bromide in water. Paper 734. Pittsburgh Conference on Analytical Chemistry and Applied Spectroscopy, Atlantic City.

McBride, M.B. 1997. A critique of diffuse double layer models applied to colloid and surface chemistry. Clays Clay Miner. 45:598–608.

Nagata, T., K. Fukushi, and Y. Takahashi. 2009. Prediction of iodide adsorption on oxides by surface complexation modeling with spectroscopic confirmation. J. Colloid Interface Sci. 332:309–316.

Petkovic, M.D., S.K. Milonjic, and V.T. Donbur. 1994. Determination of surface-ionization and complexation constants at colloidal aluminum-oxide electrolyte interface. Separ. Sci. Technol. 29:627–638.

Rhoades, J.D. 1982. Cation exchange capacity. p. 149–157. *In* A.L. Page et al. (ed.) Methods of soil analysis. Part 2. 2nd ed. Agron. Monogr. 9. ASA and SSSA, Madison, WI.

Ritter, A., R. Muñoz-Carpena, C.M. Regalado, M. Javaux, and M. Vanclooster. 2005. Using TDR and inverse modeling to characterize solute transport in a layered agricultural volcanic soil. Vadose Zone J. 4:300–309.

Seaman, J.C., P.M. Bertsch, and W.P. Miller. 1995. Ionic tracer movement through highly weathered sediments. J. Contam. Hydrol. 20:127–143.

Sims, J.T., and F.T. Bingham. 1968. Retention of boron by layer silicates, sesquioxides, and soil materials: II. Sesquioxides. Soil Sci. Soc. Am. J. 32:364–369.

Skaggs, T.H., G.V. Wilson, P.J. Shouse, and F.J. Leij. 2002. Solute transport: Experimental methods. p. 1381–1402. *In* J.H. Dane and G.C. Topp (ed.) Methods of soil analysis. Part 4. SSSA Book Series 5. SSSA, Madison, WI.

Sprycha, R. 1989a. Electrical double layer at alumina/electrolyte interface. I. Surface charge and zeta potential. J. Colloid Interface Sci. 127:1–11.

Sprycha, R. 1989b. Electrical double layer at alumina/electrolyte interface. II. Adsorption of supporting electrolyte ions. J. Colloid Interface Sci. 127:12–25.

Weerasooriya, R., and H.U.S. Wickramarathna. 1999. Modeling anion adsorption on kaolinite. J. Colloid Interface Sci. 213:395–399.

Westall, J., and H. Hohl. 1980. A comparison of electrostatic models for the oxide/solution interface. Adv. Colloid Interface Sci. 12:265–294.

Wong, M.T.F., and K. Wittwer. 2009. Positive charge discovered across Western Australian wheatbelt soils challenges key soil and nitrogen management assumptions. Aust. J. Soil Res. 47:127–135.

Zhang, P., and D.L. Sparks. 1990. Kinetics of selenate and selenite adsorption/desorption at the goethite/water interface. Environ. Sci. Technol. 24:1848–1856.